LBL--27031

DE89 012848

Keynote Address, International Workshop
on "Appropriate Methodologies for
Development and Management of
Groundwater Resources in Developing
Countries," Hyderabad, India,
February 28–March 4, 1989

A NEW APPROACH TO TRACER TRANSPORT ANALYSIS: FROM FRACTURE SYSTEMS TO STRONGLY HETEROGENEOUS POROUS MEDIA

Chin-Fu Tsang

Earth Sciences Division
Lawrence Berkeley Laboratory
University of California
1 Cyclotron Road
Berkeley, CA 94720, U.S.A.

February 1989

Most of the work upon which this report is based was done under the auspices of the Director, Office of Civilian Radioactive Waste Management, Office of Facilities Siting and Development, Siting and Facilities Technology Division, of the U.S. Department of Energy under Contract No. DE-AC03-76SF00098.

A NEW APPROACH TO TRACER TRANSPORT ANALYSIS: FROM FRACTURE SYSTEMS TO STRONGLY HETEROGENEOUS POROUS MEDIA

Chin-Fu Tsang

Earth Sciences Division
Lawrence Berkeley Laboratory
University of California
1 Cyclotron Road
Berkeley, CA 94720

ABSTRACT

Many current development and utilization of groundwater resources include a study of their flow and transport properties. These properties are needed in evaluating possible changes in groundwater quality and potential transport of hazardous solutes through the groundwater system. Investigation of transport properties of fractured rocks is an active area of research. Most of the current approaches to the study of flow and transport in fractured rocks cannot be easily used for analysis of tracer transport field data. A new approach is proposed based on a detailed study of transport through a fracture of variable aperture. This is a two-dimensional strongly heterogeneous permeable system. It is suggested that tracer breakthrough curves can be analyzed based on an aperture or permeability probability distribution function that characterizes the tracer flow through the fracture. The results are extended to a multi-fracture system and can be equally applied to a strongly heterogeneous porous medium. Finally, the need for multi-point or line and areal tracer injection and observation tests is indicated as a way to avoid the sensitive dependence of point measurements on local permeability variability.

INTRODUCTION

In the utilization and management of groundwater resources, a problem that has come into increasing attention in both developed and developing countries is the need of monitoring and maintaining groundwater quality. Thus for the long term utilization of groundwater, some of the properties of the groundwater system that should be obtained are those associated with solute (or contaminant) transport, such as effective porosity and dispersivity. These are normally obtained by tracer tests in which solutes or tracers are introduced at one location in the aquifer and its concentration on arrival measured at another location. Methods have been developed over the years to analyze such tracer transport measurements for a homogeneous porous aquifer of constant thickness, in terms of the so-called advective-dispersive equation.

The methodology becomes rather complicated if one has to deal with a heterogenous porous medium. Stochastic methods (e.g., Gelhar, 1987 and Dagan, 1987) have been developed for this if the heterogeneity is not too strong (i.e., the variance of permeability distribution in the aquifer is not large) and a representative elementary volume (REV) can be defined for the heterogeneous system. However, no methods have been fully established for a strongly heterogeneous system for which no REV can be defined. A particular type of strongly heterogeneous systems is the fractured porous medium, in which the porous medium is intersected by a system of fractures of various orientations, spacings, and sizes. This presents a difficult problem in tracer transport analysis that is being actively investigated by a number of research groups worldwide.

To put the problem in perspective, it should be pointed out that tracer transport is much more sensitive to the presence of fractures, or in general strong permeability heterogeneity, than heat transfer and pressure transmission through the system. Heat transfer is a diffusive process involving both liquid and solid components of the medium and thus often averages out formation heterogeneity. Pressure transmits effectively among fluid and solid, fracture and matrix of the medium and is also less sensitive than tracer transport to medium heterogeneity. For example, a series of connected fractures can easily form a fast path for solute transport.

The present paper attempts to introduce a new but simple model for the analysis of tracer transport for fracture systems or strongly heterogeneous porous media. The work reported is a continuing co-operation with Yvonne Tsang and Frank Hale at Berkeley and with Ivars Neretnicks and Luis Moreno at Stockholm (Tsang and Tsang, 1987; Tsang, et al., 1988a; Moreno, et al., 1988; Tsang, et al. 1988b; Tsang and Tsang, 1939; Tsang, 1989 and Tsang and Tsang, 1988). In the next section current approaches to modeling flow and transport in fractured porous media will be briefly reviewed. References are given for further study. Then results on flow and transport through single fractures will be presented. Single fractures have variable apertures and hence variable permeabilities. Thus flow through single fractures with a distribution of variable permeability is similar to the problem of flow through a two-dimensional heterogeneous porous medium. Extension of the results to multiple fractured systems will then be discussed. Finally the need of multiple-point or line/areal measurements of tracer transport is demonstrated.

CURRENT APPROACHES TO THE ANALYSIS OF FLOW AND TRANSPORT IN FRACTURED POROUS MEDIA

Three major approaches have been used to address the problem of flow and transport through fractured porous media. The first is the equivalent porous medium approach. This approach assumes that the fractures are sufficiently dense and uniformly distributed in the porous medium that the total system can be represented by a new porous medium with an effective permeability and porosity. This approach may be useful in giving average transport behavior. Recently two interesting developments have been made in this area. Pruess and co-workers (1985) considered flow of two-phase fluid in fractured porous media. Taking advantage of the fact that at low liquid saturation, the gas phase fills the fractures and the effective liquid flow permeability is that of the porous matrix and at high saturation liquid fills the fracture and thus liquid flow is dominated by fracture permeability, they are able to design an equivalent porous medium with a saturation-dependent permeability function. The other development is by Neuman (1987) who considered single phase flow in a fractured porous medium and developed a stochastic approach with permeability as a stochastic variable. The approach is applicable in the sub REV scale, i.e., applicable even if the scale of heterogeneity is such that a REV is larger than the region of study.

The second approach to modeling flow in fractured porous media is the double porosity method (Barenblatt, et al., 1960; Warren and Root, 1963; Duguid and Lee, 1977). Here the fractures and porous matrix are considered to be two overlapping continua, each with its own flow equation. The exchange between the two continua is given by a source-sink term in the two flow equations, whose magnitude is proportional to the local pressure difference between the two continua. Pruess and Narasimhan (1985) extended this into a multiple interacting continua or MINC model and successfully applied it not only to flow but also to heat transport problems. The third approach in the fracture network model (Irmay, 1964; Romm, 1966; Snow, 1965), which ignores the role of porous matrix and considers the fractures to form a network through which flow can occur. Recent work considers statistical distributions of these networks with variable fracture density, length, orientation and aperture (Long et al., 1982, 1985; Smith et al., 1987, Endo et al., 1984; Cacas et al., 1988). All the above approaches have their strengths and weaknesses. In most cases, it would be quite difficult to apply them to the analysis of tracer transport field data. A new approach is introduced in the next section.

CHARACTERIZATION OF TRACER TRANSPORT IN 2-D STRONGLY HETEROGENEOUS PERMEABLE MEDIA

The new approach is based on a detailed study of flow and transport in a two-dimensional (2-D) plane with a distribution of strongly varying permeability. This can be interpreted as an heterogeneous porous aquifer of uniform thickness or as a single fracture with variable apertures.

Most theoretical studies of fluid flow in the fractured medium make the assumption that each fracture may be idealized as a pair of parallel plates separated by a constant distance which represent the aperature of the fracture. In fact, the aperture within a rock fracture is far from being constant, and the wide range of aperture values in a single fracture gives rise to a very heterogeneous system. Hence one would expect that the fluid flow would concentrate in a few preferred paths of least fluid resistance. Evidence that flow in fractures tends to coalesce in preferred paths has been found in the field (e.g. Abelin et al., 1985; Neretnicks, 1987; and Bourke, 1987). Motivated by these data, Tsang

and Tsang (1987) proposed the variable-aperture channel model for transport through fractured media. The properties of the channel model were further developed by Tsang et al. (1988b) and the channeling characteristics of flow through a two dimensional single fracture were analyzed in detail by Moreno et al. (1988).

We use an aperture density distribution to characterize the range of aperture values in a single fracture. Based on measurement of aperture values in laboratory core samples of fracture (Gentier, 1986; Gale, 1987), we assume that the aperture values conform to a log normal distribution, which is characterized by two parameters: the mean log aperture log b_o and the standard deviation (in log b) σ_b. In addition to the aperture density distribution parameters, the spatial correlation length λ and its anisotropy ratio λ_x/λ_y (where $\lambda^2 = \lambda_x^2 + \lambda_y^2$) for the variable apertures are needed to define the fracture. Given the aperture distribution, the single fracture with variable apertures may be generated by means of standard geostatistical methods similar to a procedure described in Moreno et al. (1988), the only difference being that in that earlier work the correlation length was assumed to be isotropic.

Figure 1 show three schematic representations of the fractures so generated. Each of the three square region in Figure 1 represents a single fracture which is discretized into square meshes to which different aperture values are assigned. The five shadings used in the figure illustrate the varying aperture values in five steps from $b < 29$ μm to $b > 116$ μm, with the darkest shading representing the smallest apertures. The three realizations in Figure 1 are based on the same input log normal distribution with log $b_o = 1.7$, where the aperture b_o is in μm and $\sigma = 0.43$. They have the same correlation length $\lambda = 0.2L$, where L is the dimension of the single fracture, but different correlation anisotropy ratios of $\lambda_x/\lambda_y = 1$, 3, and 5 respectively in Figures 1a, 1b, 1c. Variograms have been computed for the apertures of all the fractures to confirm that the aperture variation obeys the required correlation length and anisotropy ratios. The increase of the correlation anisotropy ratio from 1 to 5 in the Figures 1a, 1b and 1c is also visually evident.

For the flow calculation, Darcy's law is assumed valid locally for each grid block within which the permeability is assumed to be proportional to the square of the local aperture. Then the fluid pressure at each node may be computed with a constant pressure difference maintained across the single fracture on two opposite fracture boundaries, and no flow conditions imposed on the two remaining boundaries. From the calculated fluid potential at each node, the fluid flow rate between each pair of nodes within the fracture may be computed. As an example, the flow rates so calculated for the fracture as shown in Figure 1b are displayed in Figure 2. Figure 2a shows the fluid flow when the pressure difference is applied on the left and right boundaries of the fracture and no flow boundary conditions are imposed on the top and bottom boundaries; Figure 2b shows the fluid flow when the pressure difference is applied on the top and bottom boundaries. The calculated flow rates between nodes cover a range of four orders of magnitude as a result of the log normal aperture distribution of the fracture. Five levels of shadings: space, dash line, solid line, thicker solid line and thickest solid line are used to represent the ascending values of the flow rates.

It is apparent from Figure 2 that although flow occurs in the entire plane of the fracture, the majority of flow takes place in a few selected pathways. With both geometrical configurations of boundary conditions (pressure difference from left to right and pressure difference from top to bottom), preferred paths of large flow rates are present, though the flow pattern is quite different for the two flow directions. These preferred flow paths are what we call channels, along which the apertures are variable.

Thus these channels are not large physical flow-tubes embedded in a fracture plane, but rather preferred paths, in the sense of stream-tubes in the hydraulic potential theory, due to the strong variation of the aperture and hence permeability value. The channeling effect described here occurs in addition to the physical or structural large-permeability channels in the fractured medium, such as those observed near the intersection of orthogonal fractures (Abelin et al., 1988).

We can see that the pattern of large flow rate channels (Figure 2a) observed for the boundary conditions with the pressure difference applied to the left and right boundaries is quite different from that (Figure 2b) observed for the boundary conditions of pressure difference applied to the top and bottom boundaries of the same fracture. Similar results are obtained for the fractures in Figures 1a and 1c. If the pattern of flow channeling appears to be quite different for overall flow in orthogonal directions for the same fracture, can we find parameters which are common to flow in both directions and which characterize the fluid and transport in the fracture? To study this, we calculate tracer transport through the fracture using the particle tracking method, which was first applied to study the dispersion of a heterogeneous porous medium by Smith and Schwartz (1980), and recently applied specifically to a fracture with variable apertures by Moreno et al. (1988). A sufficiently large number of particles, in our case four thousand, are introduced on the high pressure side of the fracture and are allowed to travel through the system with the probability of entering a particular flow section in the fracture proportional to the local flow rate. When a particle comes to an intersection with two or three outgoing flow sections, a Monte Carlo method is used to assign the particle to one of the flow directions with probability weighted by their respective flow rates. As each of the particle travels through the fracture, the aperture values along its flow path are recorded. These build up the statistics of the aperture values of the flow channels. Aperture density distribution functions fitted to these aperture values are shown in Figure 3. The solid line gives the probability density distribution of apertures over the entire 2D plane of the fracture. The dot-dash line and the short dash line give the aperture density distributions which describe the apertures along the actual flow paths of the particles for the boundary conditions of overall left-right flow and top-bottom flow respectively. All three curves are normalized to unit total integrated probability. Figures 3a, 3b, 3c correspond to the results for the fractures with aperture variation as shown in Figures 1a, 1b, 1c respectively.

It is clear from the distributions shown in Figure 3 that the tracer particles favor large apertures and avoid small apertures of the 2D fracture. However, they cannot avoid the small apertures altogether and thus there is a finite probability of flow through apertures one or two orders of magnitudes smaller than the large apertures most particles travel through. The result is that solute transport is described by a distribution function that is different from that of the 2D fracture: the former has a larger mean k value and a smaller standard deviation (see Figure 3). The point that tracer transport is described by a distribution with a larger mean k value can be illustrated in the special limiting case of a fully stratified medium where the permeabilities, k, of the layers obey a lognormal distribution. With the layers in parallel, the number of tracer particles are proportional to k in each layer, so that the tracer particles see the set of k values that is the original lognormal distribution weighted by k. The weighted distribution function turns out also to be lognormal with the mean log k increased by $\sigma^2 \ln 10$, where σ is the standard deviation of log k.

Now Figure 3 also shows that the aperture distribution functions along the channels are almost identical for the two orthogonal flow geometries (left-right and top-bottom flows). This is not obvious a priori, since the channels in the two cases represent rather different flow paths (Figure 2a and 2b). The result is even less obvious when one considers that the anisotropy ratio of the correlation length is a factor of 5 for the case in Figures 1c and 3c. We believe the insensitivity of the aperture values of the flow paths in the two orthogonal directions of overall flow arises from the fact that the correlation length chosen here is 0.2L. That is, the scale of heterogeneity is on the order of one fifth of the flow region or measurement scale, and effects of boundaries and stratification are not significant. Hence the correlation length is small enough for the particles flowing under different boundary conditions to sample statistically similar values of aperture along the flow paths. In the limit that the scale of heterogeneity is increased to the size of the flow region, then the large anisotropy ratio in the aperture correlation length would give rise to a highly stratified medium through which the flow should consist of major conduits of very large apertures in the direction parallel to the large correlation length, but many smaller apertures are sampled in the orthogonal direction. When this happens, the aperture density distribution of the particle flow paths will be very sensitive to the geometric configuration of the boundary conditions. But as long as the spatial correlation length is reasonably small (less than 1/5 of the measurement), we believe that even over a range of anistropy ratios of the correlation, flow characteristics in terms of aperture distributions (Figure 3) are the same in the two directions. Thus we arrive at the interesting result that channels of tracer transport in the fracture system is characterized by an aperture density distribution function, independent of specific deterministic flow paths, or the anisotropy ratio, as long as the correlation length of the heterogeneity is not too large.

The above discussions were presented in terms of flow and transport through a single fracture with variable aperture. The discussion could also easily be expressed for a strongly heterogeneous porous medium defined by a permeability probability distribution where the scale of heterogeneity is expressed in terms of a correlation length in the spatial variation of k. In our single fracture calculations, the variable is the fracture aperture b which relates to the local permeability by the relation $k = b^2/12$. In the porous medium, the fluid volumetric flow rate is proportional to kA, where A is the cross sectional area to the flow. Thus, the equivalent kA varies as $b^3/12$. A wide range of values in kA would give rise to the phenomenon of channeling. Therefore all the above observations for the fluid flow behavior in a single fracture with variable aperture is directly applicable to a highly heterogeneous porous medium (one with a strong spatial variation in permeability). One may then make the following remarks. The heterogeneous medium would give rise to flow channeling, and provided that the largest scale of heterogeneity is less than a few tenths of scale of measurement, the least resistive channels for tracer transport are characterized by a permeability distribution, which differs from the permeability distribution of the entire medium. The distribution along the channel typically takes on a larger mean and a smaller spread. Therefore, the dispersion of the system is not related to the spread of the permeability distribution over the entire region, but rather to the spread of the subset of permeability values along the preferred flow channels. (See Figure 3.)

EXTENSION TO MULTI-FRACTURE SYSTEMS

A multi-fracture system is composed of a network of intersecting single fractures. A simple example is shown in Figure 4. Since within each single fracture, the flow

channeling occurs as demonstrated in the last section, transport through the multiple fracture system is also through channels as is apparent in this figure. If all the fractures in the multi-fracture system have the same basic properties geologically, i.e., they can be related to the same aperture density distribution, the channelled transport through the multi-fracture system is characterized by the same particle-path aperture density distribution with its mean log b_0 and spread σ_b. If the fractures in the system are composed of two, three or more sets of fractures, each related to its own aperture density distribution, then the aperture density distribution characterizing the tracer transport through the system will be a composite, or union, of all the distributions for the different sets. An example of channeling flow in a series of 2 fractures is shown in Figure 5. It is easy to see that such calculations can be done to many connected fractures. We have obtained results for up to 100 fractures in series.

DEPENDENCE OF TRACER TRANSPORT AND CONCENTRATION BREAKTHROUGH CURVES ON PERMEABILITY VARIANCE

In the last section we demonstrated that tracer transport through a fracture system is characterized by a mean aperture, log b_0 and the spread σ_b in log b. This can be directly translated to permeability distribution by the equation $kA \sim b^3$, with the associated mean and permeability spread σ_k in log k. In this section the dependence of flow and transport through a heterogeneous system as a function of σ_k is presented. Given the permeability distribution function and a spatial correlation length we can generate as before a realization of permeability spatial distribution as shown in Figure 6. This figure corresponds to the case of $\sigma_k = 1.29$ and $\lambda = 0.1$, and is shown in a contour plot form. A pressure difference is then applied to the left and right boundaries, while the top and bottom boundaries are closed. The flow lines are calculated and represented in Figure 7a-d by arrows at each location with the sizes of the arrows proportional to the logarithm of local flow rates. Figure 7c is the result of flow field for the heterogeneous system in Figure 6. If the value of σ_k is changed, the flow is strongly affected. Figure 7a,b,c and d shows the results for $\sigma_k = 0.3$, 0.6, 1.29 and 1.8 respectively. The change of flow field from the almost uniform flow to channeled flow corresponds to low σ_k (almost constant k) case to large σ_k as the strongly heterogeneity case. This is even more apparent when we plot the flow rates along the exit line for these 4 cases (Figure 8).

Now a tracer transport calculation is done by particle tracking method. The permeability probability distribution of the 2D distribution and that along the particle paths are shown in Figure 9 for two different values of $\sigma_k = 0.6$ and 1.29. The curves for $\sigma_k = 0.6$ is narrower than that for $\sigma_k = 1.29$, and the shift between particle path and the 2D distribution is also smaller for the smaller σ_k value. According to the last section it is these particle-path permeability probability distribution functions that characterize the tracer transport.

The particle tracking method affords us also a way to calculate the tracer concentration breakthrough curves along the exit line on the right side of Figure 6. A step function of concentration is applied by introducing tracer particles on the left side and collected along the right boundary. This is done for a number of realizations of the permeability distribution. The results are shown in Figure 10 for two values of $\sigma_k = 0.6$ and $\sigma_k = 1.29$, with four realizations in each case. Thus more dispersion (a larger initial slope) is noticed for larger input σ_k. The band covering the different realizations for each σ_k value represents the intrinsic uncertainties of these curves due to statistical variability. The above calculation was made assuming the porosity, ϕ, of the heterogeneous porous medium to be constant. For a single fracture of variable aperture, the spread in porosity

or aperture (and hence the spread of pore velocity) is related to that of permeability by $\sigma_\phi = \sigma_k/3$. The results of these two assumptions on porosity are compared in Figure 11. It is interesting to note that the constant ϕ case has more dispersion for the concentration breakthrough curves.

Given either a constant porosity or a variable porosity with a finite value of σ_ϕ, the tracer breakthrough curves such as those shown in Figure 10 can be correlated with σ_k, a parameter characterizing the heterogeneous medium. Such an approach has been applied with some success to a few sets of field data. (See: Tsang et al., 1988b and Tsang and Tsang, 1988.)

THE NEED FOR MULTIPLE-POINT OR SPATIALLY AVERAGED RESULTS FOR TRACER TRANSPORT

So far we have considered tracer transport through a heterogeneous system with tracer injection along the left boundary line and tracer observation along the right boundary line of the system. However often point tracer injection and observation are made. For heterogeneous systems, this kind of measurement may not be adequate since tracer transport through the medium is strongly dependent on local variations of permeability and porosity. In other words, if one makes point measurements in which the measurement (or sample) size is less than or comparable to the spatial correlation length of the variability, the result is so sensitive to statistical variations that it is cannot be analyzed.

To illustrate this, consider tracer transport between two sides of a single fracture with variable aperture shown in Figure 6. the spatial correlation length, λ, in this particular case is 0.1 L, where L is the linear dimension of the fracture. Assuming a pressure difference is applied on the two sides of the fracture, flow is established with paths shown in Figure 12, where the thickness of the lines are drawn as proportional to the square root of the local flow rates.

Now, let tracer particles be released only within a section length $s < L$ at a few high-flow locations along the high pressure side and collected at a few high-flow positions on the low pressure side (see Figure 13). The collection length is also assumed to be s. Calculations were made for $s/L = 0.1, 0.2, 0.3,...,0.8$. Figure 14 shows tracer breakthrough curves for $s/L = 0.1$ for one of the realizations with $\lambda/L = 0.1$. Here tracers are released at two alternative locations, A and b, and collected at three alternative locations, D, E and F (Figure 13). These locations are chosen because of their relatively large local flow rates. At each section, concentration, C, was calculated by dividing the accumulative exit particle number by the local flow rate. The maximum input concentration, C_o, is defined as the total number of tracer particles used in the calculation divided by the flow rate in the input section. The plot in Figure 14 is C/C_o versus time of arrival t, at the exit sections. Note that C/C_o does not reach a value of 1 because of mixing of water from the tracer-injection section with the remainder of water inflow from the high pressure side. Also in this figure, only five curves are shown, though there are six possible flow connections. The reason is that the flow from point B to point D is so slow that its first arrival time is out of the range of this graph.

Several comments on the calculations may be made. First, the exit flow rates at the three exit sections are quite different. They are given by $Q = 26, 53, 37$ units, respectively. Second, the initial arrival times of the six possible tracer paths do not correlate with the linear distances between the tracer-injection section and the collection section. For

example, the earliest arrival time corresponds to the case with linear transport of 1.04 L (from B to E), and this is about half of the arrival time for a case with a slightly shorter linear transport distance of 1.005 L (from B to F). Such non-correlation between initial arrival times and linear transport distances has often been observed in the field. A recent example may be found in data from the Fanay-Augeres field tracer experiment (Cacas et al., 1988).

One may define a measure for the dispersion displayed in Figure 14 as given by $(t_{0.9} - t_{0.1})/t_{0.5}$, were t_x is the time of arrival when the concentration reaches a fraction x of the maximum concentration value at large times. This empirical definition of dispersion has the advantage that it is independent of a model for the system. Taking the cases shown in Figure 13, and calculating the value of the dispersion measure as defined above for each case, the results obtained are spread out over a factor of 3 from each other (see Figure 15 for s = 0.1 L). However, carrying out the same exercise with the tracer collection section length increased from s/L = 0.1 to 0.8 in steps of 0.1, the spread of the dispersion measure is greatly reduced. This is shown in Figure 15.

The results in Figure 15 suggest that line measurements with line section lengths corresponding to a few correlation lengths may yield less sensitive values for the dispersion measure, which may then be the appropriate predictive quantity for the model.

This study suggests that formation heterogeneity can result in calculated tracer transport dispersivity with large uncertainties. Such uncertainties, however, can be greatly reduced if the consideration is not transport between points but rather those between line or areal tracer sources and observations, where these line or areas cover two or more spatial correlation lengths of the heterogeneity. In other words, such averaging or summation reduces significantly the statistical range of predicted dispersivity values. Thus, it is perhaps impossible to predict the tracer concentration at a point in space at an instant of time. However, it may be possible to predict, within a reasonable range of uncertainty, tracer transport behavior between a region of tracer sources and an observation region. In many problems of current interest, such as the performance assessment of a nuclear waste repository, perhaps this is what is required.

CONCLUSIONS AND SUMMARY

In this paper we reviewed briefly the current approaches in the modeling of flow and transport in fractured rocks. A detailed study of the permeability heterogeneity of a single fracture shows a channeling behavior of tracer transport which can be extended to a multi-fracture rock system. Results of the study apply also to flow and transport through a strongly heterogeneous porous medium. Two major conclusions may be given as follows:

(1) Heterogeneity in fractures and also in porous media gives rise to flow channeling effects. Tracer transport through these flow channels can be characterized by a permeability probability distribution function. The mean of this distribution function is larger than that of the permeability probability function over the entire 2-D heterogeneous medium. Tracer concentration breakthrough curves can then the analyzed to obtain the parameters (mean and variance) of the permeability probability distribution function.

(2) Since this is a statistical approach to interpret tracer transport data, it is shown that it would be impossible to make accurate predictions of concentration of tracer arrival at a point in time and space, due to local permeability variations. It is demonstrated that multiple-point or line/areal measurements of tracer transport should be made over a few spatial correlation lengths, that would average the variability and may yield dispersion parameter characteristic of the medium. In other words, this new approach may not be able to make point predictions of tracer transport, but may be able to predict tracer concentration over a region of space. In many practical applications, perhaps this capability is all that is required.

ACKNOWLEDGEMENTS

Continued co-operation and discussions with F.V. Hale, Y.W. Tsang, L. Moreno and I. Neretnicks are much appreciated. Comments and discussions on the manuscript from T.N. Narasimhan, P. Bideau, and L. Myer are gratefully acknowledged. Most of the work on which this report is based was performed under the auspices of the Office of Facilities Siting and Development, Siting and Facilities Technology Division, the Office of Civilian Radioactive Waste Management of the Department of Energy through contract number DE-AC03-76SF00098.

REFERENCES

Abeline, H., Bergersson, L., Gidlund, J., Moreno, L., Neretnieks, I., Widen, H., and Andersson, J., 1988. Results of some large scale in situ tracer experiments in a drift at the Stripa Mine, Proceedings of International Conference on Fluid Flow in Fractured Rocks, Atlanta, Georgia, May 16–18, 1988.

Abeline, H., Neretnieks, I., Tunbrant, S. and Moreno, I., 1985. Final report on the migration in a single fracture, Experimental results and evaluations, Sven. Kärnbränslefösorjning Tech. Report. 85-03, Nucl. Fuel Safety proj., Stockolm.

Barenblatt, G.I., Zheltov, I.P., and Kochina, I.N., 1960. Basic concepts in the theory of seepage of homogeneous liquids in fissured rocks (strata): PMM, Vol. 24, No. 5, p. 852–864; English translation, Applied Mathematics and Mechanics, Vol. 24, p. 1286–1303, 1960.

Bourke, P.J., 1987. Channeling of flow through fractures in rock. Proceedings of GEOVAL-87, International Symposium, Stockholm, Sweden, April 7–9, 1987.

Cacas, M.C., Ledoux, E., and de Marsily, G., 1988, Calibration and validation of a three-dimensional stochastic network model on a large scale experiment with flow measurements and tracer tests performed in the uranium mine of Fanay-Augeres, Proceedings of International Conference on Fluid Flow in Fractured Rocks, Atlanta, Georgia, May 16–18, 1988.

Dagan, Gedeon, 1987. Review of stochastic theory of transport in groundwater flow, in Groundwater Flow and Quality Modelling, E. Custodio, A. Gurgui and J.P. Lobo-Ferreira, Editors, Reidel Publishers, Dordrecht, The Netherlands, pp. 1–32.

Duguid, J.O., and Lee, P.C.Y., 1977. Flow in fractured porous media. Water Resources Research, Vol. 13, No. 3, p. 558–566.

Endo, H.K., Long, J.C.S., Wilson, C.R. and P.A. Witherspoon, 1984. A model for investigating mechanical transport in fractured networks, Water Resources Research, Vol. 200, No. 10, pp. 1390-1440.

Gale, J.E., 1987. Comparison of coupled fracture deformation and fluid flow models with direct measurements of fracture pore structure and stress-flow properties, Proceedings of 28th U.S. Symposium of Rock Mechanics, Tuscon, Arisona, 19 June-1 July, p. 1213–1222.

Gelhar, L.W., 1987, Stochastic analysis of solute transport in saturated and unsaturated porous media, in Advances in Transport Phenomena in Porous Media, Jacob Bear and M. Yavnz Corapcioglu, Editors, Martinus Nijhoff Publishers, Dordrecht, The Netherlands, pp. 657–700.

Gentier, S., 1986. Morphologie et comportment hydromecanique d'une fracture naturelle dans un granite sous contrainte normale, Doctoral Thesis, U. d'Orleans, France.

Irmay, 1964. Theoretical models of flow through porous media. RILEM Symp. on the Transfer of Water in Porous Media, Paris, April.

Long, J.C.S., Gilmour, P., and Witherspoon, P.A., 1985. A Model for steady fluid flow in random three-dimensional networks of disc-shaped fractures, Water Resources Research, Vol. 21, No. 8, pp. 1105–1115.

Long, J.C.S., Remer, J.S., Wilson, C.R., and Witherspoon, P.A., 1982. Porous media equivalents for networks of discontinuous fractures, Water Resources Research, Vol. 18, No. 3, pp. 645–658.

Moreno, L., Tsang, Y.W., Tsang, C.F., Hale, F.V., and Neretnieks, I., 1988. Flow and tracer transport in a single fracture: A stochastic model and its relation to some field observation, Water Resources Research, Vol. 24, No. 12, pp. 2033–3048.

Neretnieks, I., 1987. Channeling effects in flow and transport in fractured rocks—some recent observations and models, Proceedings of GEOVAL-87, International Symposium, Stockholm, Sweden, April 7–9, 1987.

Neuman, Shlomo, P., 1987. Stochastic continuum representation of fractured rock permeability as an alternative to the REV and fracture network concepts, in Groundwater Flow and Quality Modelling, E. Custodio, A. Gurgui and J.P. Lobo-Ferreira, Editors, Reidel Publishers, Dordrecht, The Netherlands, pp. 331–362.

Pruess, K. and Narasimhan, T.N., 1985. A practical method for modeling fluid and heat flow in fractured porous media, Society of Petroleum Engineering Journal, Vol. 25, No. 1, pp. 14–26.

Pruess, K., Tsang, Y.W., and Wang, J.S.Y., 1985. Modeling of strongly heat-driven flow in partially saturated fractured porous media, in Proceedings of Conference on Hydrogeology of Rocks of Low Permeability, Tucson, Arizona, pp. 486–497.

Romm, E.S., 1966. Fluid flow in fractured rocks, Nedra, Moscow.

Smith, L., Schwartz, F., and Mase, C., 1987. Applications of stochastic methods for the simulation of solute transport in discrete and continuum models of fractured rock systems, Proceedings of Conference on Geostatistical, Sensitivity and Uncertainty Methods for Ground-Water Flow and Radionuclide Transport Modeling, San Francisco, California, September 15–17, 1987, pp. 425–440.

Smith, L. and Schwartz, F.W, 1980. Mass transport. 1, A stochastic analysis of macroscopic dispersion, Water Resources Research, Vol. 16, No. 2, pp. 303–313.

Snow, D.T., 1965. A parallel model of fractured permeable media. Ph.D. Thesis, University of California, Berkeley, 330 p.

Tsang, C.F., 1989. Tracer travel time and model validation, International Journal of Radioactive Waste Management and the Nuclear Fuel Cycle, in press.

Tsang, C.F., Tsang, Y.W., and Hale, F.V., 1988a. Tracer transport in fractured rocks, Invited Paper, Proceedings of the International Conference in Flow in Fractured Rocks, Atlanta, Georgia, May 16–18, 1988.

Tsang, Y.W. and Tsang, C.F., 1987. Channel model of flow through fractured media, Water Resources Research 23(3), 467–479, 1987.

Tsang, Y.W. and Tsang, C.F., 1988. Interpretation of large scale tracer transport by a multi-fracture channel model, EOS. Transactions of the American Geophysical Union, Vol. 69, No. 44, p. 1176.

Tsang, Y.W. and Tsang, C.F., 1989. Flow Channeling through strongly heterogeneous media. Submitted to Water Resources Research, January, 1989.

Tsang, Y.W., Tsang, C.F., Neretnieks, I., and Moreno, L., 1988b. Flow and tracer transport in fractured media—A variable aperture channel model and its properties, Water Resources Research, Vol. 24, no. 12, pp. 2049–206.

Warren, J.E. and Root, P.J., 1963. The behaviour of naturally fractured reservoirs, Soc. Petrol. Eng. J., Vol. 3, p. 245–255.

FIGURE CAPTIONS

Figure 1. Statistically generated apertures with spatial correlation length of 0.2L in the plane of a single fracture of linear dimension L. The aperture values are partitioned into five classes with the smallest apertures corresponding to the darkest shading. The three realizations have different anisotropy ratio for the spatial correlation length: (a) $\lambda_x/\lambda_y = 1$, (b) $\lambda_x/\lambda_y = 3$, and (c) $\lambda_x/\lambda_y = 5$.

Figure 2. Fluid flow rates for the fracture with aperture variations as shown in Figure 1b. The thickness of the lines is proportional to the flow rates. Pressure difference is applied from (a) left to right, and (b) top to bottom.

Figure 3. The aperture probability density distributions for apertures over the 2D fracture, along flow paths with left-right pressure difference, and along flow paths with top-bottom pressure difference for the fractures shown in (a) Figure 1a, (b) Figure 1b, and 9c) Figure 1c.

Figure 4. Schematic picture of three intersecting fractures with flow channeling

Figure 5. Flow channeling in two intersecting fractures. Aperture distribution is shown on top and flow lines are shown in the bottom.

Figure 6. Highly heterogeneous 2-D porous medium with contours in log k.

Figure 7. Flow through the heterogeneous system shown in Figure 6, with rates proportional to arrow sizes for four different values of permeability standard deviation $\sigma_k = 0.3, 0.6, 1.29, 1.8$.

Figure 8. Exit flow rates at different points along the exit line corresponding to Figure 7, for $\sigma_k = 0.3, 0.6, 1.29, 1.8$.

Figure 9. Comparison of permeability probability distribution function in 2D medium with that along particle flow paths, for $\sigma_k = 0.6$ and 1.29.

Figure 10. Tracer breakthrough curves for $\sigma_k = 0.6$ and $\sigma_k = 1.29$. Four realizations are shown for each σ_k value. Figure 6 is the permeability plot for one of the four realizations with $\sigma_k = 1.29$.

Figure 11. Tracer breakthrough curves for a heterogeneous medium shown in Figure 6, using two assumptions of porosity variability: $\sigma_\phi = 0$ and $\sigma_\phi = \sigma_k/3$.

Figure 12. Fluid flow rates for the fractures with aperture variations as shown in Figure 6. The thickness of the lines is proportional to the square root of the flowrates. Pressure difference is applied from left to right.

Figure 13. Schematic diagram illustrating "point" measurements of tracer transport. Based on one of the realizations of a fracture with variable apertures with an applied left-right pressure difference, tracers are deposited at A and B and collected at D, E, and F. Points A, B, D, E and F are chosen at locations of large entrance or exit flow rates and each is associated with a section length of 0.1L.

Figure 14. Tracer breakthrough curves for cases shown in Figure 13, with the section length for tracer entrance or exit equal to 0.1L.

Figure 15. The tracer dispersion, measured as the standard deviation of particle residence times, as a function of the section length for tracer entrance or exit. At each S/L value the points represent results from different alternative injection-collection pairs.

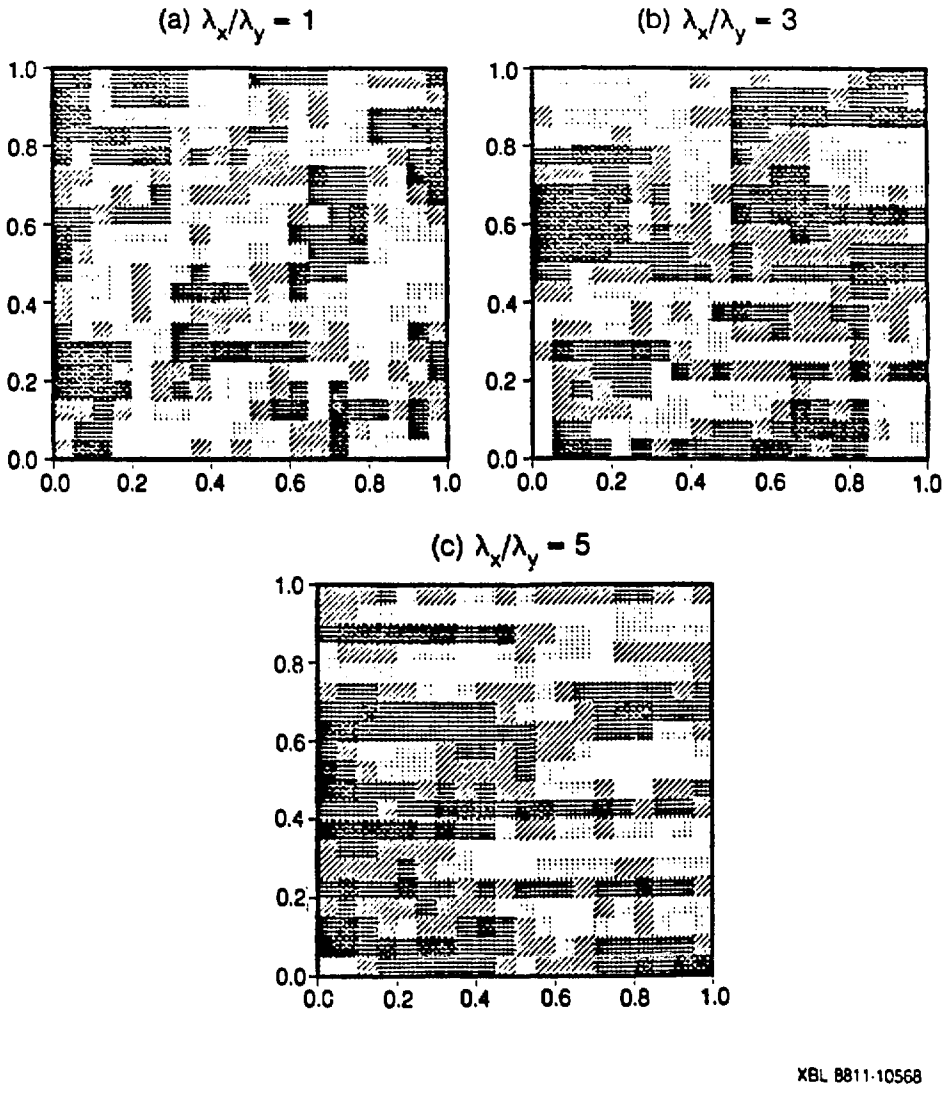

Figure 1. Statistically generated apertures with spatial correlation length of 0.2L in the plane of a single fracture of linear dimension L. The aperture values are partitioned into five classes with the smallest apertures corresponding to the darkest shading. The three realizations have different anisotropy ratio for the spatial correlation length: (a) $\lambda_x/\lambda_y = 1$, (b) $\lambda_x/\lambda_y = 3$, and (c) $\lambda_x/\lambda_y = 5$.

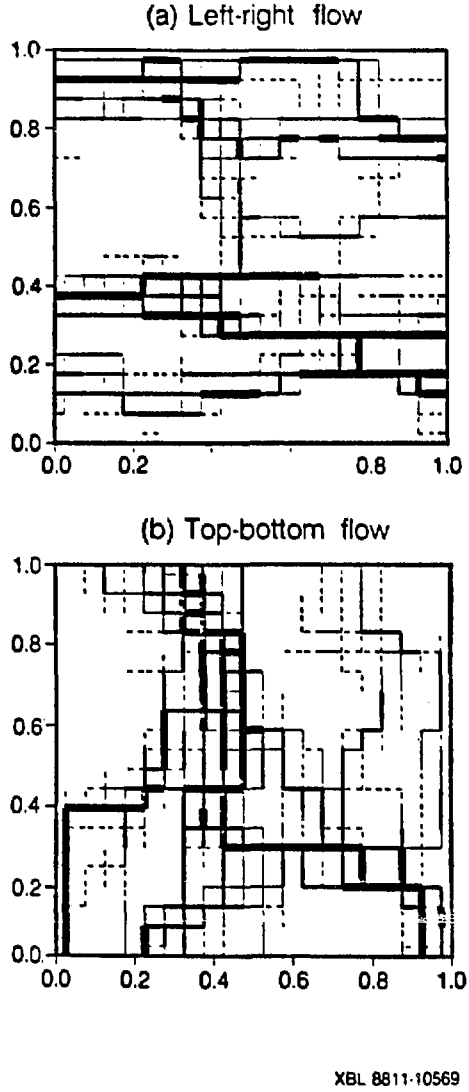

Figure 2. Fluid flow rates for the fracture with aperture variations as shown in Figure 1b. The thickness of the lines is proportional to the flow rates. Pressure difference is applied from (a) left to right, and (b) top to bottom.

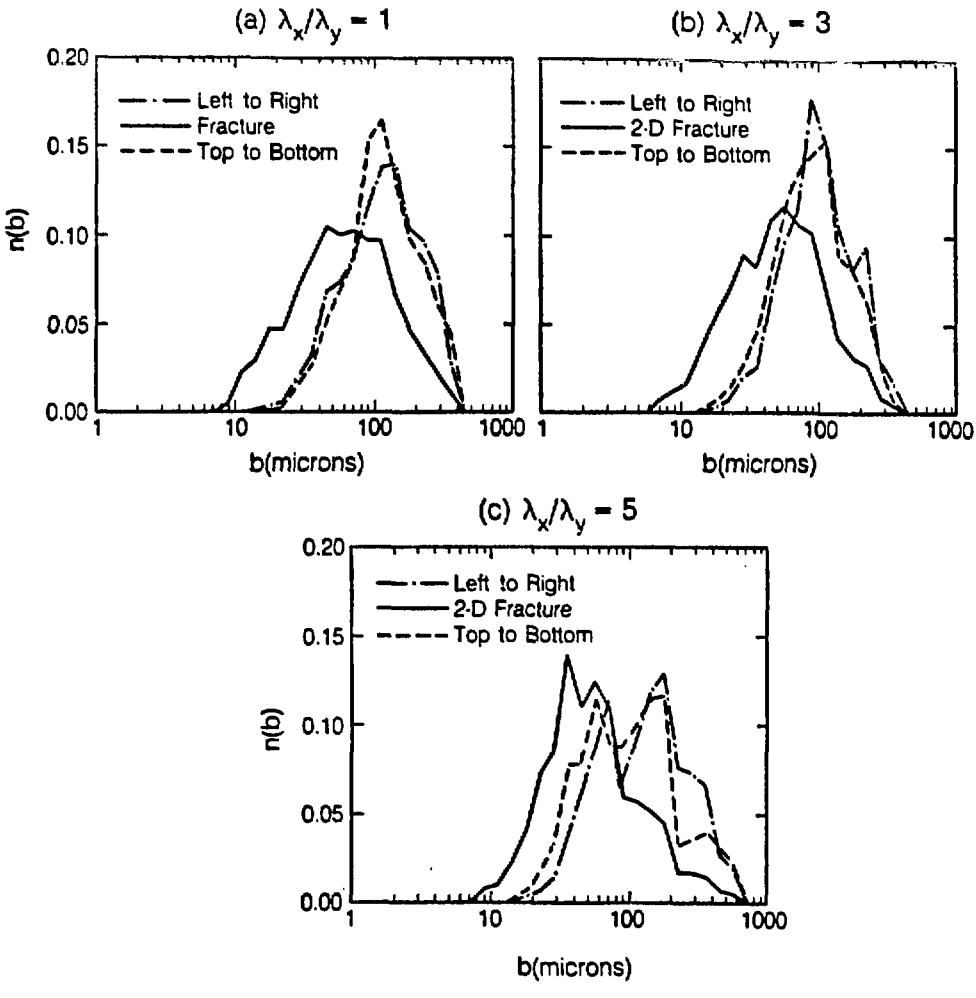

Figure 3. The aperture probability density distributions for apertures over the 2D fracture, along flow paths with left-right pressure difference, and along flow paths with top-bottom pressure difference for the fractures shown in (a) Figure 1a, (b) Figure 1b, and 9c) Figure 1c.

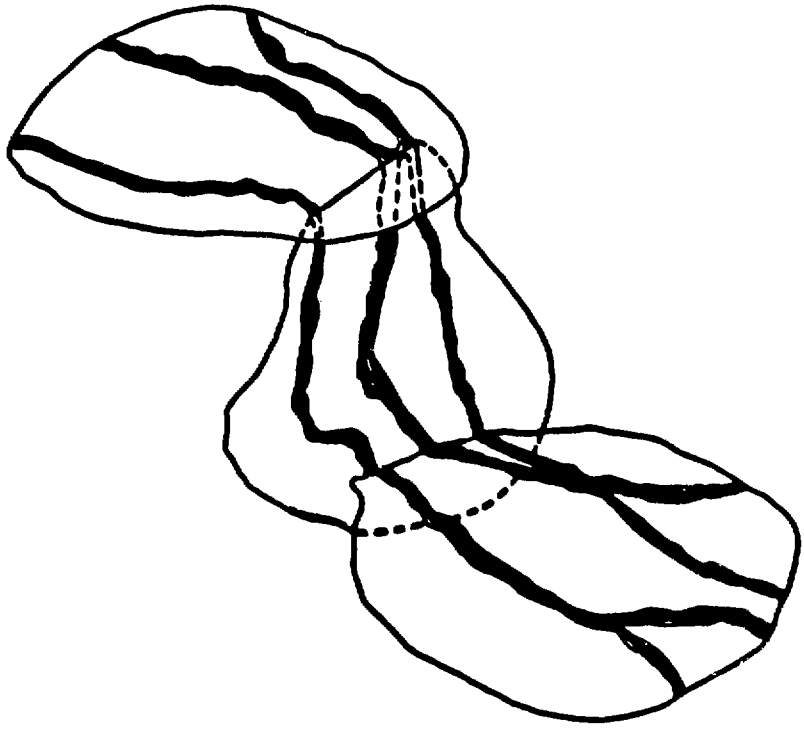

Figure 4. Schematic picture of three intersecting fractures with flow channeling

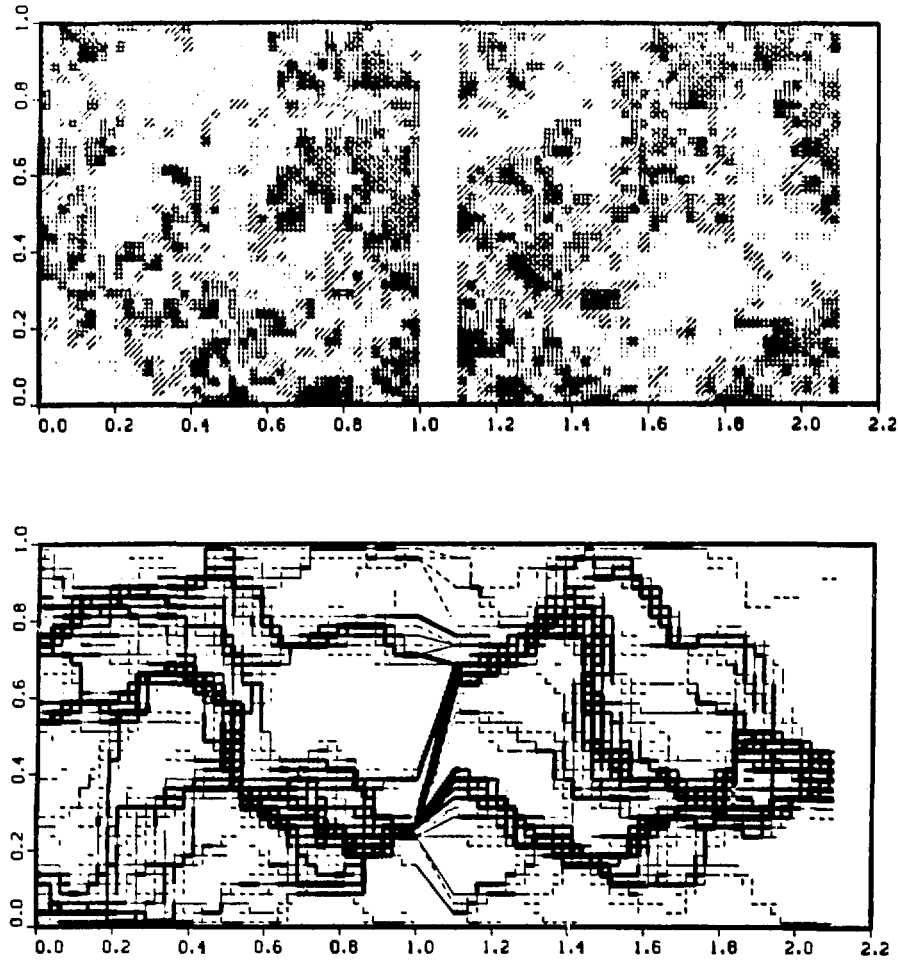

Figure 5. Flow channeling in two intersecting fractures. Aperture distribution is shown on top and flow lines are shown in the bottom.

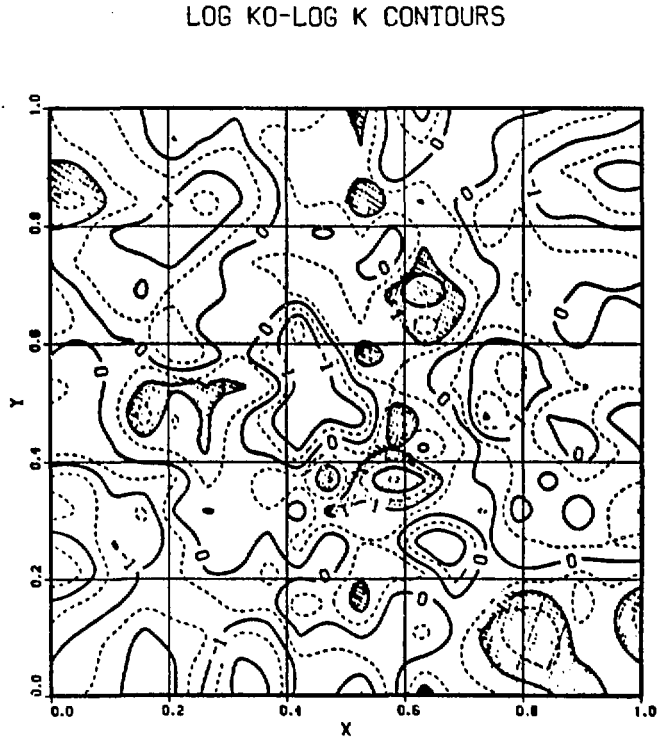

Figure 6. Highly heterogeneous 2-D porous medium with contours in log k.

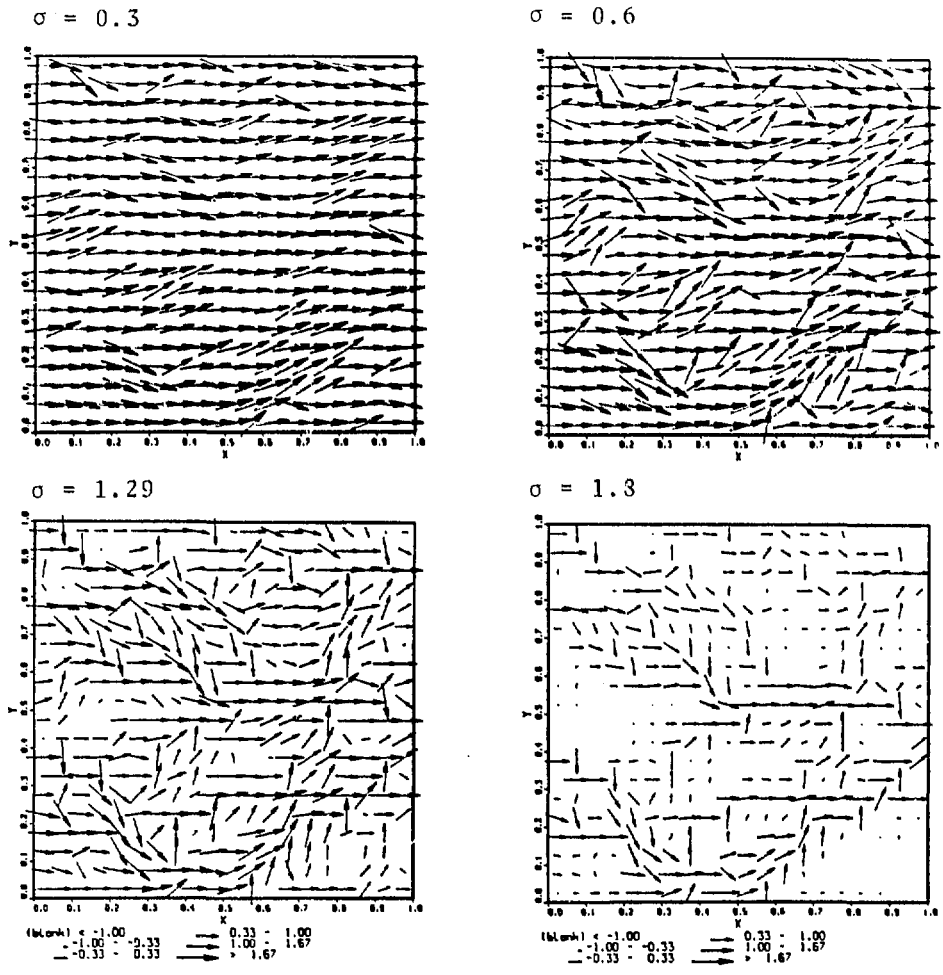

Figure 7. Flow through the heterogeneous system shown in Figure 6, with rates proportional to arrow sizes for four different values of permeability standard deviation σ_k = 0.3, 0.6, 1.29, 1.8.

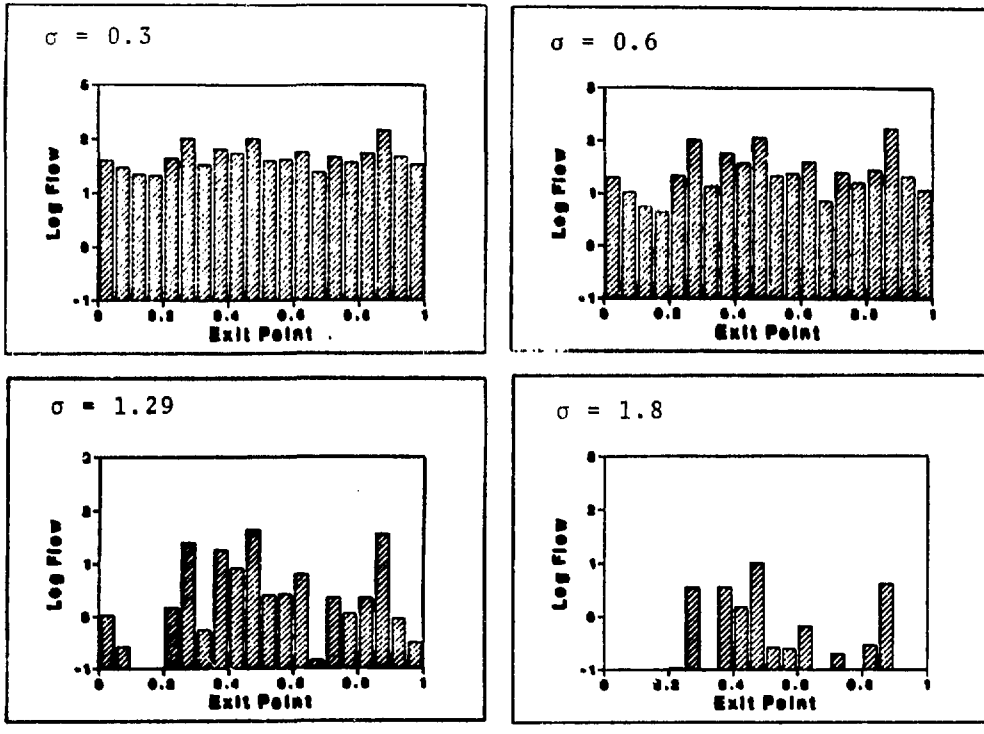

Figure 8. Exit flow rates at different points along the exit line corresponding to Figure 7, for $\sigma_K = 0.3, 0.6, 1.29, 1.8$.

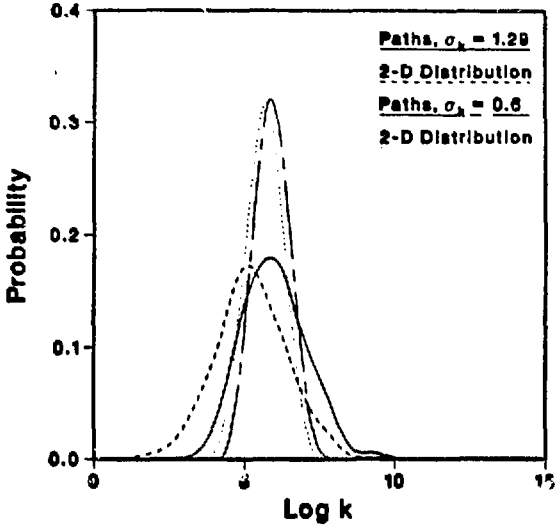

Figure 9. Comparison of permeability probability distribution function in 2D medium with that along particle flow paths, for σ_k = 0.6 and 1.29.

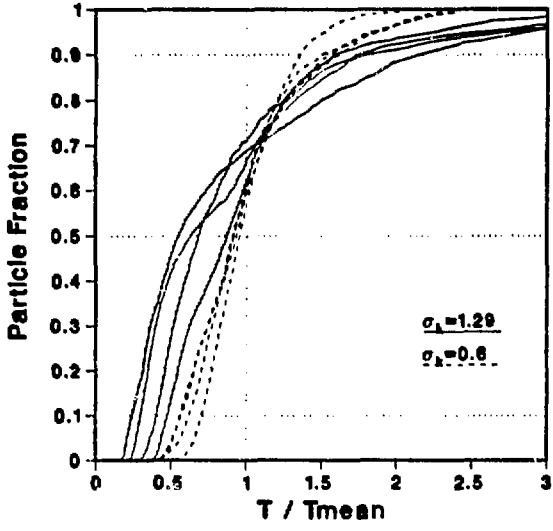

Figure 10. Tracer breakthrough curves for σ_k = 0.6 and σ_k = 1.29. Four realizations are shown for each σ_k value. Figure 6 is the permeability plot for one of the four realizations with σ_k = 1.29.

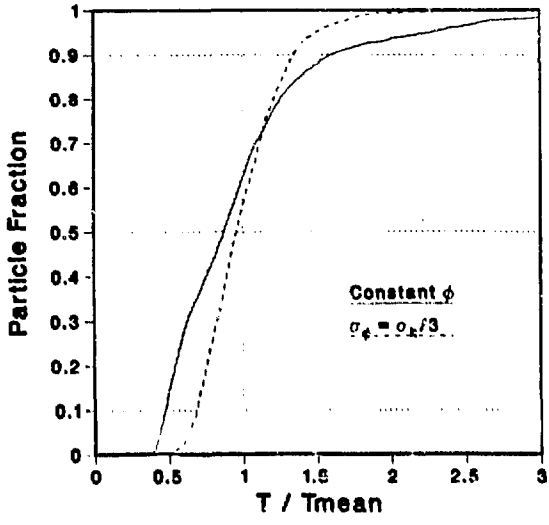

Figure 11. Tracer breakthrough curves for a heterogeneous medium shown in Figure 6, using two assumptions of porosity variability: $\sigma_\phi = 0$ and $\sigma_\phi = \sigma_k/3$.

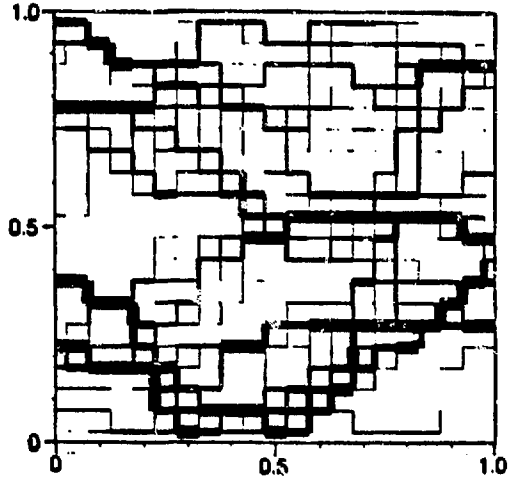

Figure 12. Fluid flow rates for the fractures with aperture variations as shown in Figure 6. The thickness of the lines is proportional to the square root of the flowrates. Pressure difference is applied from left to right.

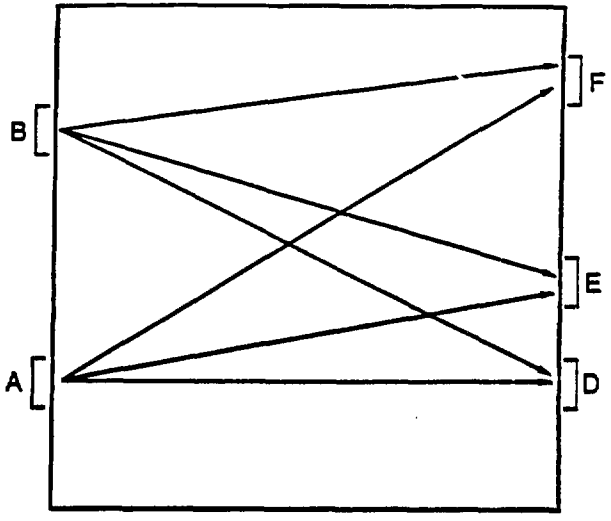

Figure 13. Schematic diagram illustrating "point" measurements of tracer transport. Based on one of the realizations of a fracture with variable apertures with an applied left-right pressure difference, tracers are deposited at A and B and collected at D, E, and F. Points A, B, D, E and F are chosen at locations of large entrance or exit flow rates and each is associated with a section length of 0.1L.

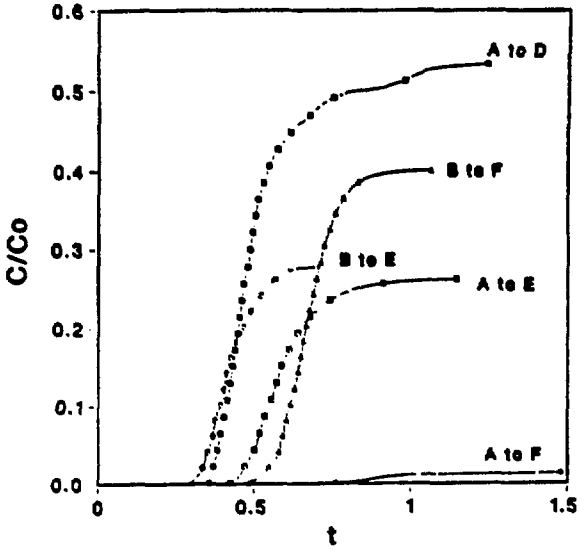

Figure 14. Tracer breakthrough curves for cases shown in Figure 13, with the section length for tracer entrance or exit equal to 0.1L.

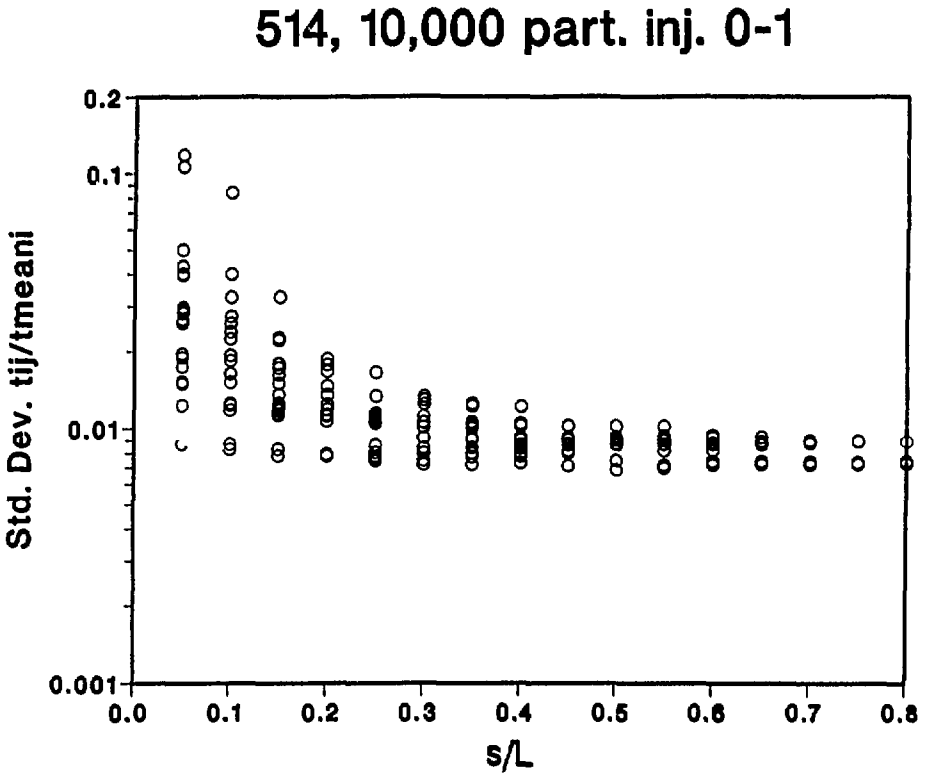

Figure 15. The tracer dispersion, measured as the standard deviation of particle residence times, as a function of the section length for tracer entrance or exit. At each S/L value the points represent results from different alternative injection-collection pairs.